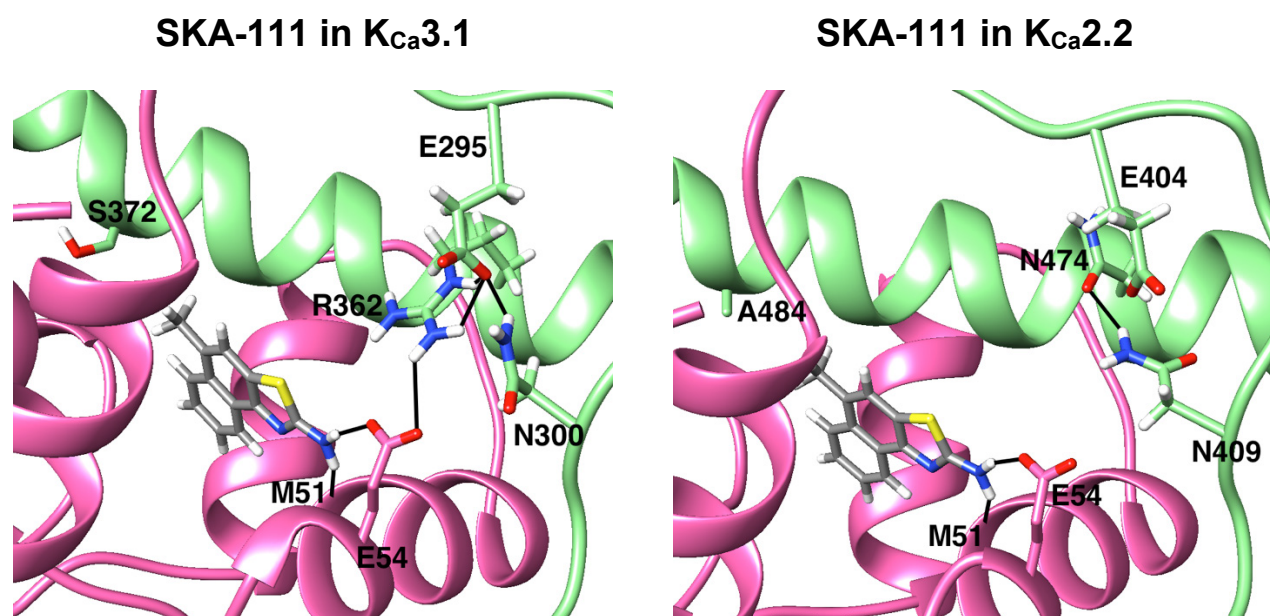


Supplementary Fig.1



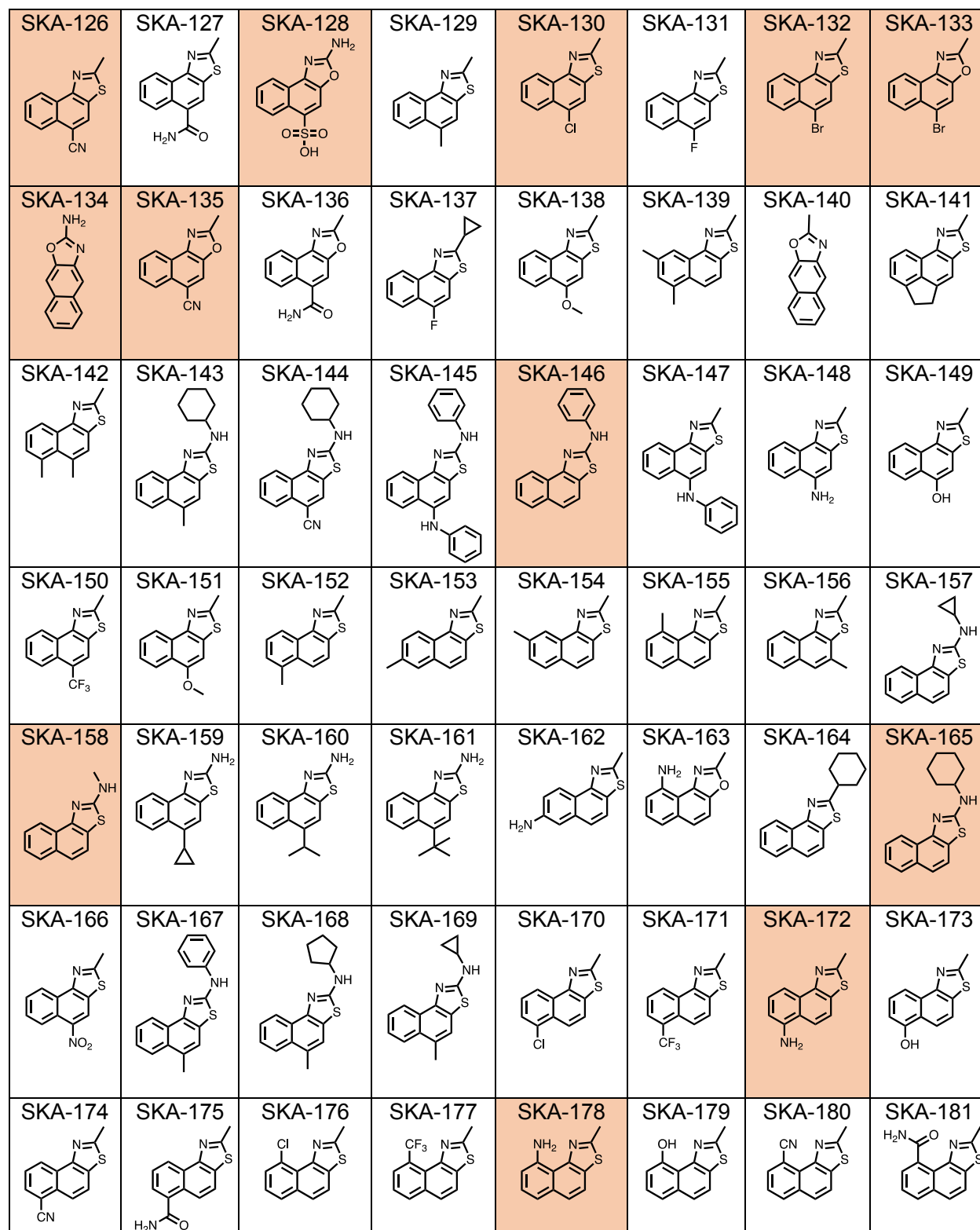
Docking model of K_{Ca}3.1 and K_{Ca}2.2 CaM-BD/CaM complexes with SKA-111. In the K_{Ca}3.1 model the amino group of the benzothiazole ring system of SKA-111 forms hydrogen bonds with M51 and E54 in calmodulin. E54 is further stabilized by an extensive hydrogen bond network with R362, E295 and N300 in the K_{Ca}3.1 channel model, which we hypothesized to be responsible for the 100-fold K_{Ca}3.1 selectivity of SKA-111. In the K_{Ca}2.2 model, however, SKA-111 forms only hydrogen bonds with M51 and E54. Due to the shorter length of the N474 side chain in K_{Ca}2.2 E54 is not stabilized by additional hydrogen bonds. The CaM-BD is shown in light green; CaM is colored pink.

The eight 2-aminobenzothiazoles shown below, which all display some degree of selectivity for K_{Ca}3.1 over K_{Ca}2 channels, converged on similar binding poses as SKA-111 with an extensive hydrogen bond network centered around R362 in the K_{Ca}3.1 model and hydrogen bonds between the -NH₂ group and M51 and E54 in CaM in both the K_{Ca}3.1 and the K_{Ca}2.2 model.

SKA-31	SKA-44	SKA-45	SKA-72	SKA-73	SKA-107	SKA-117	SKA-120

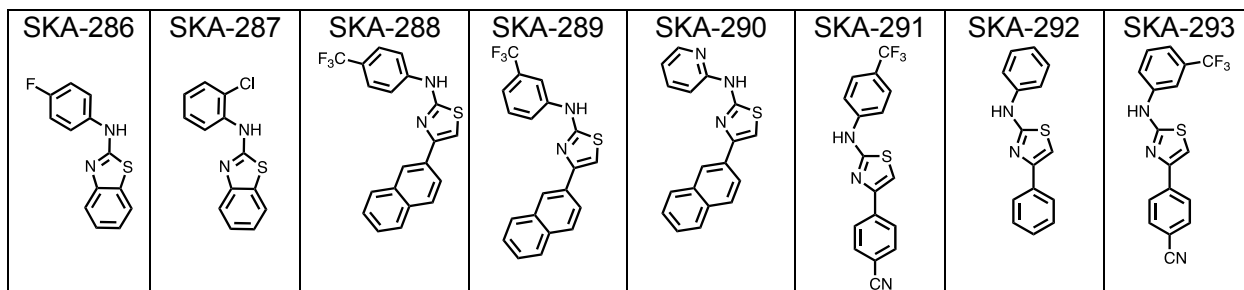
Supplementary Fig.2

Chemical structures of the 168 virtually designed and docked compounds. Highlighted compounds were synthesized and tested.



SKA-182 	SKA-183 	SKA-184 	SKA-185 	SKA-186 	SKA-187 	SKA-188 	SKA-189
SKA-190 	SKA-191 	SKA-192 	SKA-193 	SKA-194 	SKA-195 	SKA-196 	SKA-197
SKA-198 	SKA-199 	SKA-200 	SKA-201 	SKA-202 	SKA-203 	SKA-204 	SKA-205
SKA-206 	SKA-207 	SKA-208 	SKA-209 	SKA-210 	SKA-211 	SKA-212 	SKA-213
SKA-214 	SKA-215 	SKA-216 	SKA-217 	SKA-218 	SKA-219 	SKA-220 	SKA-221
SKA-222 	SKA-223 	SKA-224 	SKA-225 	SKA-226 	SKA-227 	SKA-228 	SKA-229
SKA-230 	SKA-231 	SKA-232 	SKA-233 	SKA-234 	SKA-235 	SKA-236 	SKA-237

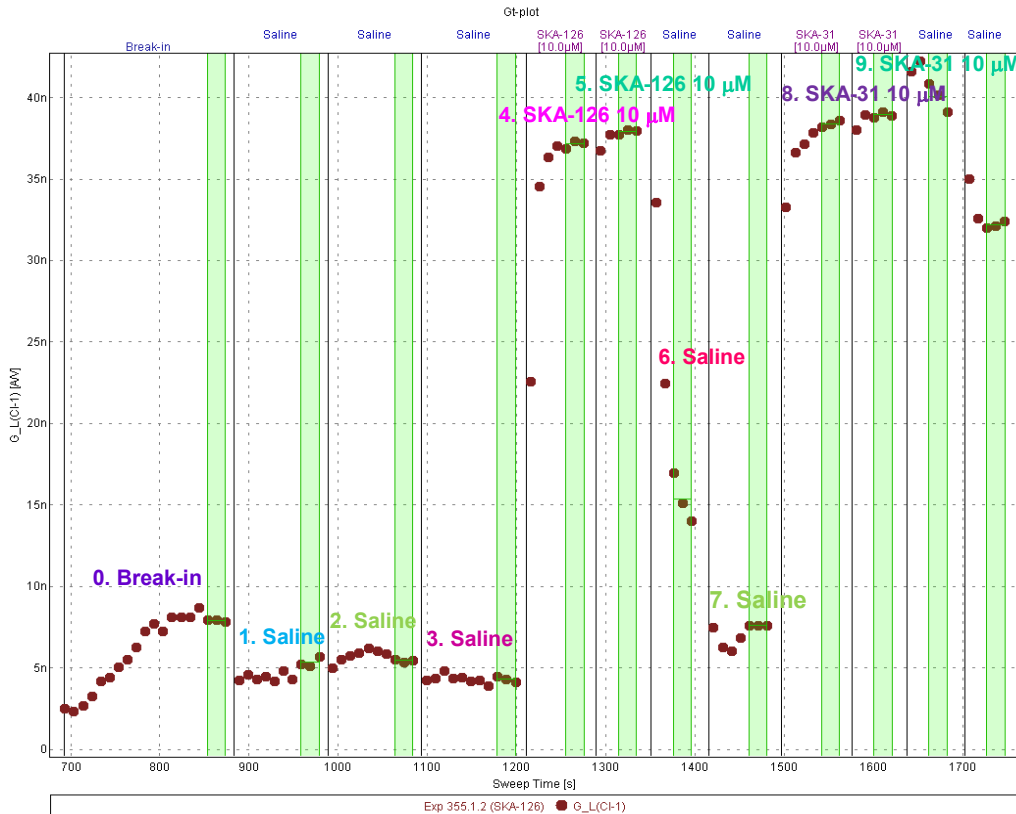
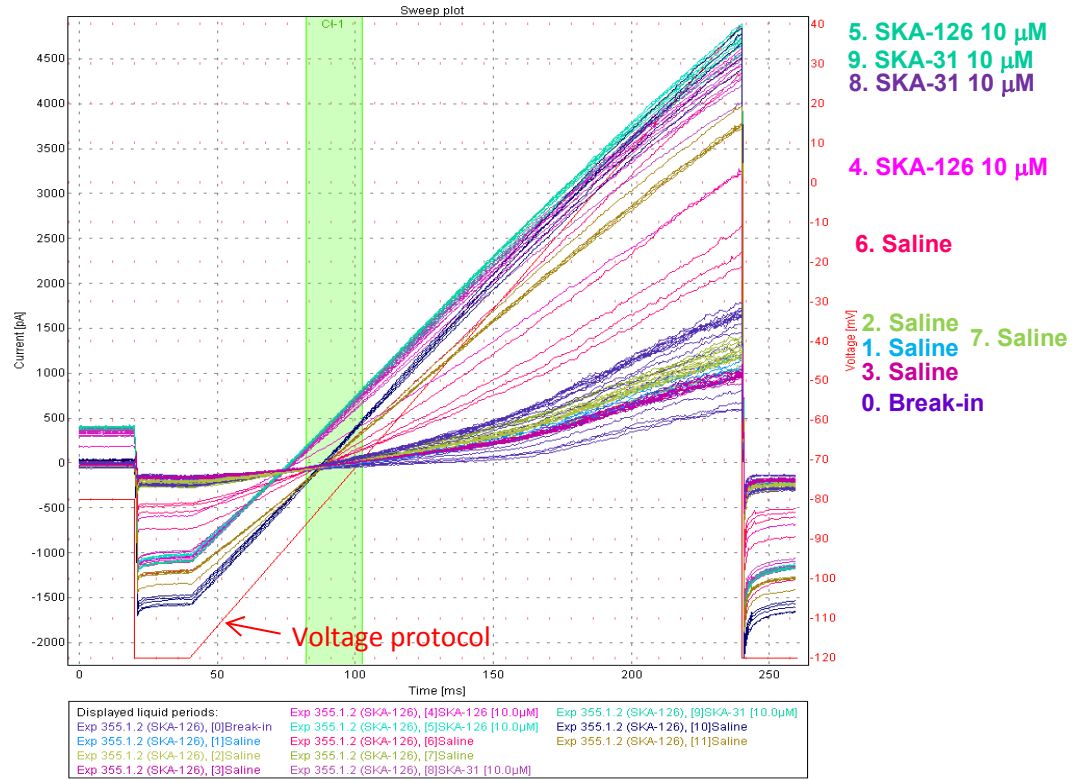
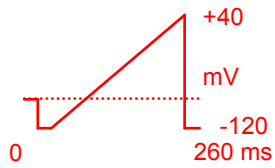
SKA-238 	SKA-239 	SKA-240 	SKA-241 	SKA-242 	SKA-243 	SKA-244 	SKA-245
SKA-246 	SKA-247 	SKA-248 	SKA-249 	SKA-250 	SKA-251 	SKA-252 	SKA-253
SKA-254 	SKA-255 	SKA-256 	SKA-257 	SKA-258 	SKA-259 	SKA-260 	SKA-261
SKA-262 	SKA-263 	SKA-264 	SKA-265 	SKA-266 	SKA-267 	SKA-268 	SKA-269
SKA-270 	SKA-271 	SKA-272 	SKA-273 	SKA-274 	SKA-275 	SKA-276 	SKA-277
SKA-278 	SKA-279 	SKA-280 	SKA-281 	SKA-282 	SKA-283 	SKA-284 	SKA-285



Supplementary Fig.3

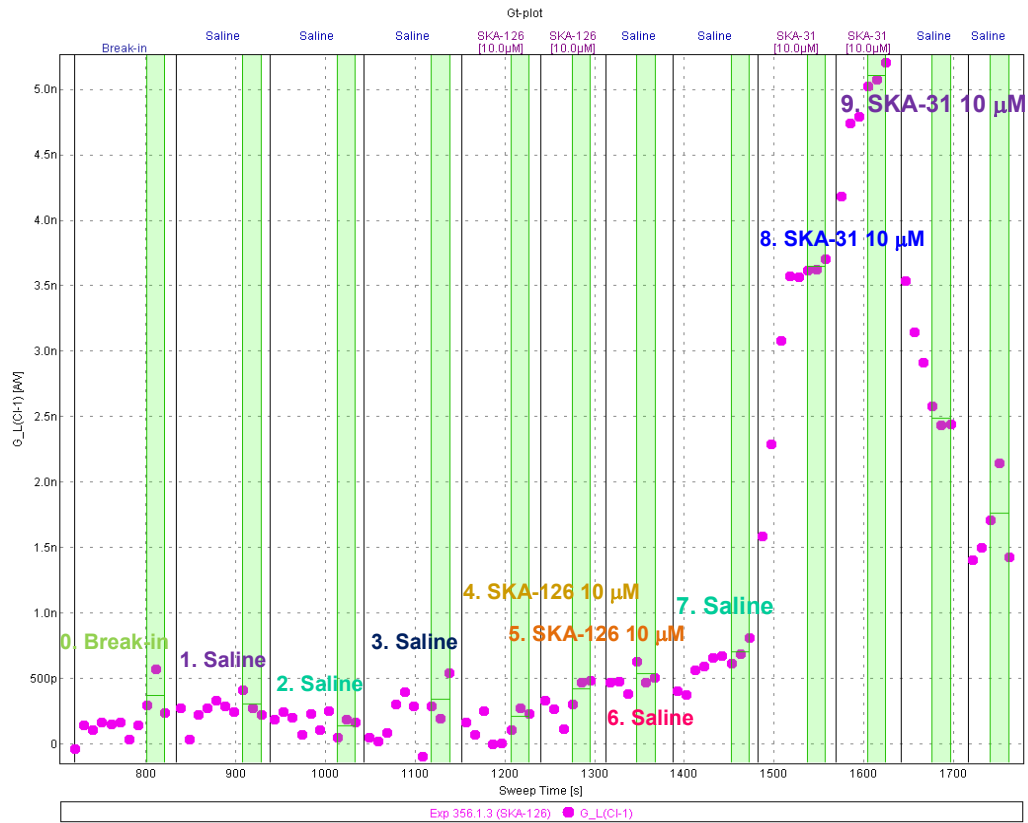
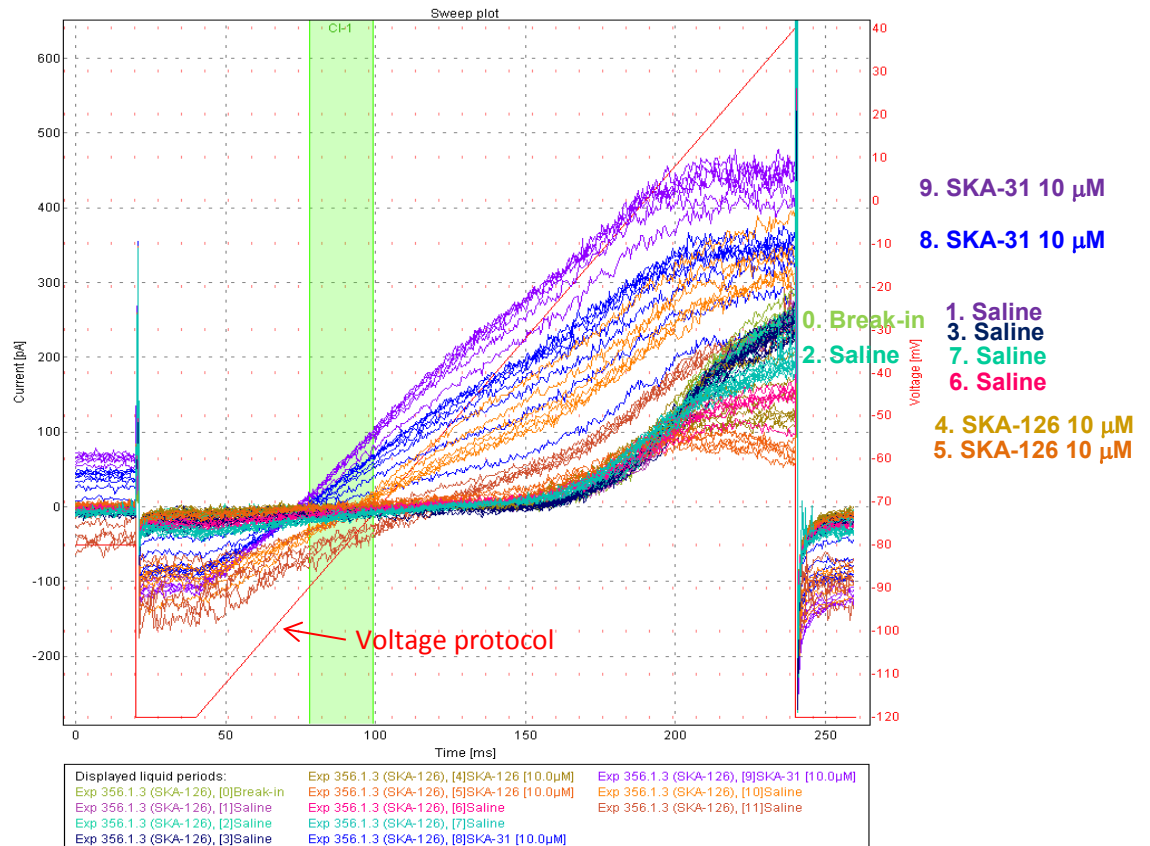
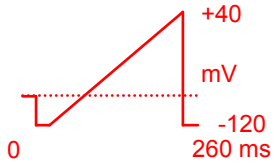
QPatch screening of activator compounds on $K_{Ca3.1}$ and $K_{Ca2.2}$ channels with 250 nM of free Ca^{2+} in the internal solution.

Screening of SKA-126 on $K_{Ca3.1}$



Raw current traces (top) and plot of current slope (measured between -85 and -65 mV) versus time for K_{Ca} activation (bottom). SKA-31 was used as the positive control. Saline or drugs were perfused during the first 15 sec of each so-called liquid period.

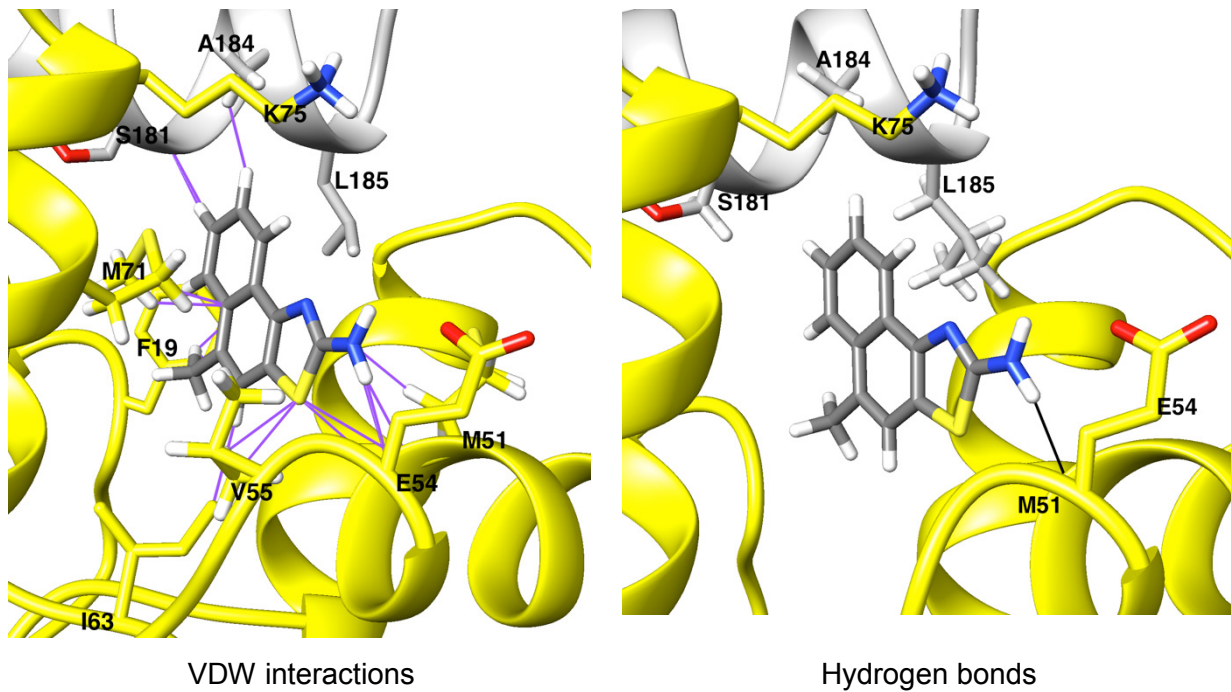
Screening of SKA-126 on $K_{Ca2.2}$



Raw current traces (top) and plot of current slope (measured between -85 and -65 mV) versus time for K_{Ca} activation (bottom). SKA-31 was used as the positive control.

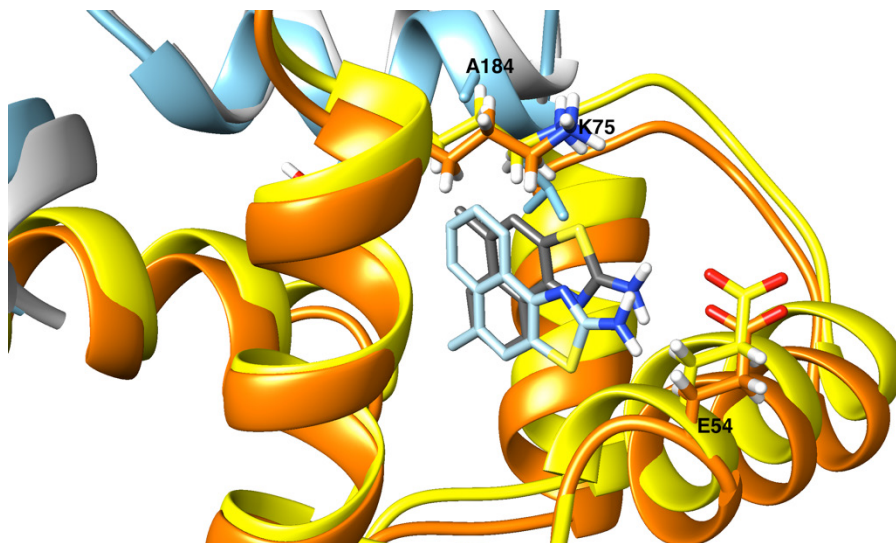
Note: $K_{Ca2.2}$ currents are smaller than $K_{Ca3.1}$ currents and show some rectification at positive potentials.

Supplementary Fig.4



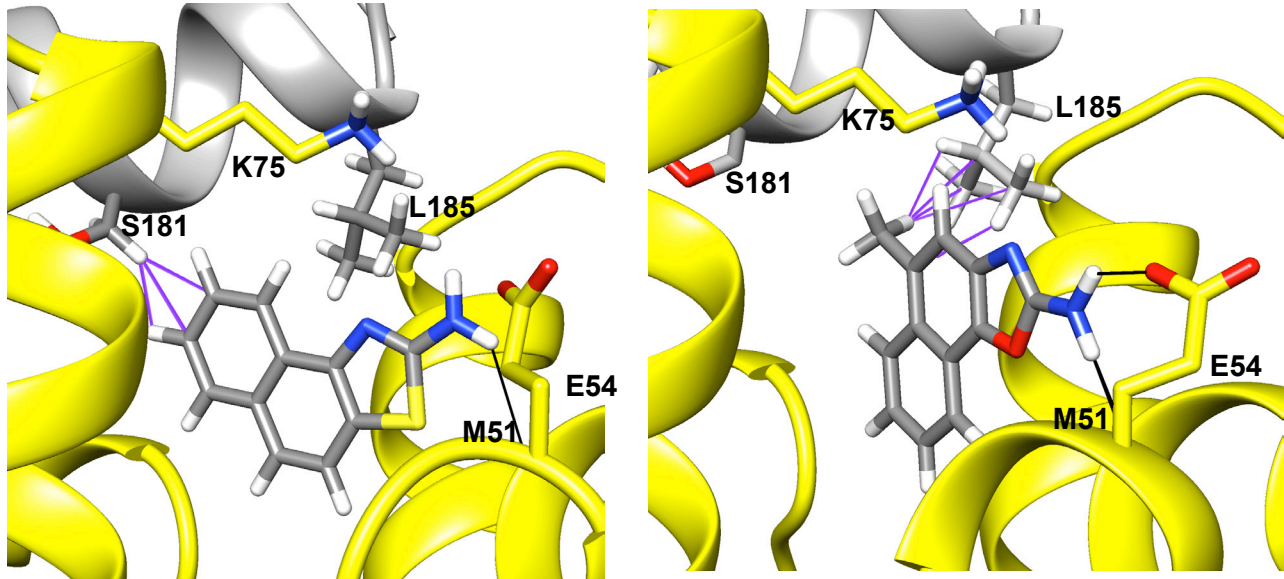
SKA-111 in $K_{Ca}3.1$ open state 2 (pdb id: 6cno)

The channel is shown in gray and the CaM N-lobe in yellow. Hydrogen bonds are shown in black, van der Waals interactions are visualized in purple. SKA-111 forms one hydrogen bond with M51 (right) and makes 12 van der Waals contacts with residues in the $S_{45}A$ helix and the CaM N-lobe (left).



Overlay of the Rosetta docking models of SKA111 in open state 1 (yellow and light grey) and open state 2 (orange and sky blue). SKA-111 is shown in dark grey in open state 1 and in light blue in open state 2.

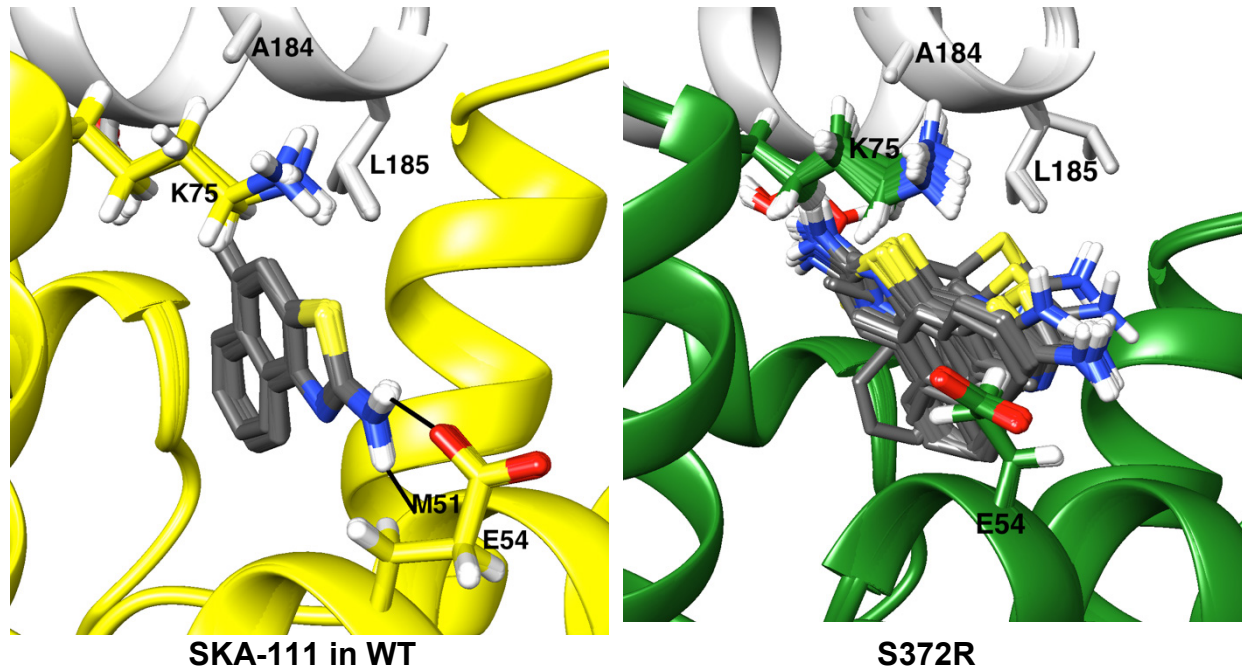
Supplementary Fig.5



SKA-31 (left) and SKA-121 (right) in KCa3.1 open state 1 (pdb id: 6cnn)

The channel is shown in gray and the CaM N-lobe in yellow. Hydrogen bonds are shown in black, van der Waals interactions are visualized in purple. For clarity, not all side chains of CaM residues within contact range of ligand are explicitly shown.

Supplementary Fig.6



Rosetta ligand docking models of the top 50 lowest energy-binding poses of SKA-111 in the interface between the CaM N-lobe (yellow: WT, green: S372R) and the S₄₅A helix (light gray) of wild type KCa_{3.1} and the S372R KCa_{3.1} mutant. Molecular docking shows that SKA-111 converged well in wild type KCa_{3.1} but not in the S372R KCa_{3.1} mutant channel.